Analysis of power losses and voltage variation by the V2G system penetration in the radial low-voltage feeder

Peerapon Chanhom[1*], Chusak Khumpim[1] and Peerasak Paopang[1]

Abstract

This research analyzes the line power losses and voltage variation that are caused by the V2G system penetration in the study power network. The V2G system is demonstrated as mathematical model, and simulated by the computer program for investigating the relationship among the line power losses, voltage variation, and probability of the V2G location. The 3 cases study of the V2G penetration are presented and assigned to describe the behavior of charging and discharging the amount of active power by the V2G system. The simulation results show large amount of line power losses and voltage variation issues can be found in case of the congestion of discharging power is closely occurred to the distribution transformer and the end of power distribution network. However, these issues can be overcome by distributing the charging or discharging location of the V2G system. The relationship earlier mentioned can clearly depict by the proposed variation index.

Keywords: vehicle-to-grid, plug-in electric vehicles, power losses, voltage variation.

[1] Faculty of Industrial Education, Rajamangala University of Technology Suvarnabhumi, Nonthburi 11000

[*] Corresponding author. E-mail: peerapon.c@rmutsb.ac.th

Introduction

Vehicle-to-Grid (V2G) is a smart system that the grid utility can communicate with the plug-in electric vehicles i.e., battery electric vehicles (BEVs) and plug-in hybrids electric vehicles (PHEVs), through the smart communication system. To operate the V2G system, the aggregator is the necessary service, where it works as a commercial distributor between the utility and the multiple BEVs/PHEVs owners instead of the grid utility communicating with individual BEV/PHEV (Cleveland and Morris, 2006). By the available storages of V2G, the grid utility can buy the stored energy from the BEVs/PHEVs during the peak hours, and sell it back when the demand is low (Zhu, 2015). Nowadays, the V2G system has acquired much attention amongst power system engineers, and numerous attractive business models have been proposed (Sortomme and El-Sharkawi, 2012). While interconnecting of the V2G system with the power network for reverse the power flow (discharging mode) seems able to gain the benefit from an energy arbitrage (Liu *et al.*, 2013), the challenge is how efficient (or inefficient) is the process of integrating the V2G system to the power network (Dehaghani and Williamson, 2012). Modeling a real-time operating condition for the V2G power flow and detailed analysis of relationship among the power losses, voltage variation, and the V2G

location are necessary, and these are provided in this research. A new variation index is proposed to depict the relationship.
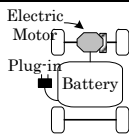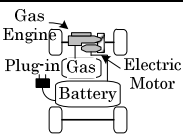
Methodology

Electric vehicles technologies

Many types of vehicles are powered by electricity, and available in the market i.e., fuel cell electric vehicles (FCEVs), hybrid electric vehicles (HEVs), PHEVs, and BEVs (IEA, 2013). Among these, PHEVs and BEVs have a capable to operate the V2G system by communicating with the smart communication system through the on-board plug-in (Kong and Karagiannidis, 2016). The characteristics of PHEVs and BEVs are mainly summarized in (Table 1).

Numerous of charging stations were deployed around the world, and there are the well-known standards, SAE J1772 and IEC 62196. These standards mainly specify the safety devices and charging systems. The charging systems however can simply be summarized in the (Table 2). The charging connector includes the control signaling, not only allowing control of local charging, but allowing the electric vehicles to participate in a wider electric vehicle network. As (Table 2), regular charging is charging with low current approximately 16-32 A (3.3-7.4 kW), but quick charging is charging with relatively high current approximately 63 A (43 kW 3-phase) for only 30 minutes.

Table 1 BEVs and PHEVs comparison.

	BEVs	PHEVs
propulsion, energy source and system.	Electric Motor / Plug-in / Battery	Gas Engine / Plug-in(Gas) / Battery / Electric Motor
characteristic	- zero emission	- very low emission
	- short range	- long range
major issues	- charging facilities	- multiple energy source control

Numerous of charging stations were deployed around the world, and there are the well-known standards, SAE J1772 and IEC 62196. These standards mainly specify the safety devices and charging systems. The charging systems however can simply be summarized in the (Table 2). The charging connector includes the control signaling, not only allowing control of local charging, but allowing the electric vehicles to participate in a wider electric vehicle network. As (Table 2), regular charging is charging with low current approximately 16-32 A (3.3-7.4 kW), but quick charging is charging with relatively high current approximately 63 A (43 kW 3-phase) for only 30 minutes.

Table 2 Charging technologies.

	quick	regular
charging time	30-min	8-14-hr
input voltage	200 V 3-phase	200 V 1-phase
hardware	in quick charge	on board
comm. system	CAN	no

V2G modeling and control

In this research, the V2G system has been demonstrated into the mathematical model for investigating the power losses and voltage variation by the V2G system penetration. The details of modeling and control of the V2G system will be provided. (Figure 1) shows the example of single line diagram of the V2G system. The V2G can be modeled, and composed of a voltage source converter (VSC), a DC-link, and a controller unit. Normally, the VSC is connected in parallel with a power distribution system at the point of common coupling (PCC) through the coupling inductor

(L). The reactive reactance of this inductor (X_L) is act as the passive filtering of the switching harmonic distortion generated by the VSC. Basically, the active and reactive power (P, Q) can be injected into or drawn from the power distribution system by controlling amplitude and phase angle of the V2G voltage ($V_{v2g} \angle \delta$) respected to the PCC voltage (V_{pcc}), which can be expressed by

$$P = \frac{V_{v2g} V_{pcc} \sin \delta}{X_L} \qquad (1)$$

$$Q = \frac{\left(V_{v2g} \cos \delta - V_{pcc} \right) V_{pcc}}{X_L} \qquad (2)$$
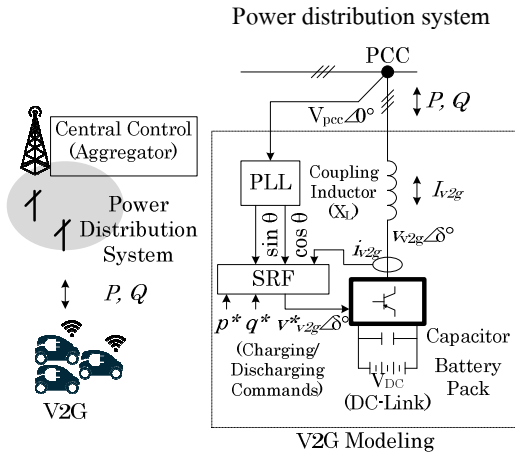

Figure 1 The single line diagram of the V2G system.

where, P is active power generated by the V2G,

Q is reactive power generated by the V2G,

V_{v2g} is voltage of the V2G,

V_{pcc} is voltage of the PCC,

δ is phase angle between V_{pcc} and V_{v2g}, and

X_L is inductive reactance of the coupling inductor.

From (1) and (2), operating modes of the V2G can be explained by the P-Q chart illustrated in (Figure 2). It can be found the V2G can both operate in P and Q mode at the same time. However, in this research, the V2G system is considered in only +P and –P operating modes. The purpose is to analyze the power losses and voltage variation corresponding to the charging or discharging demands of the electric vehicle's battery.

To understand the V2G control system, the details of the control state space of the V2G modeling will be explained. This is necessary to clarify the method to control the amount of charging and discharging active power of the V2G system. Consider the coupling voltage and generating current including, the PCC voltage (V_{pcc}), the V2G voltage (V_{v2g}), and the V2G current (I_{v2g}) illustrated in (Figure 1 and 2) These elements can be expressed into the alternating current (AC) 3-phase coordinates (ABC and abc) as

$$V_{pcc} = \begin{bmatrix} V_A \\ V_B \\ V_C \end{bmatrix} \qquad (3)$$

$$V_{v2g} = \begin{bmatrix} V_a \\ V_b \\ V_c \end{bmatrix} \quad (4)$$

$$I_{v2g} = \begin{bmatrix} I_a \\ I_b \\ I_c \end{bmatrix} \quad (5)$$

From (3) to (5), I_{v2g} is charging or discharging current corresponding to the different amplitude and phase angle of V_{v2g} respect to V_{pcc} through the coupling inductor (L), which can be presented by

$$\frac{d}{dt}\begin{bmatrix} I_a \\ I_b \\ I_c \end{bmatrix} = \frac{1}{L}\begin{bmatrix} V_a - V_A \\ V_b - V_B \\ V_c - V_C \end{bmatrix} \quad (6)$$
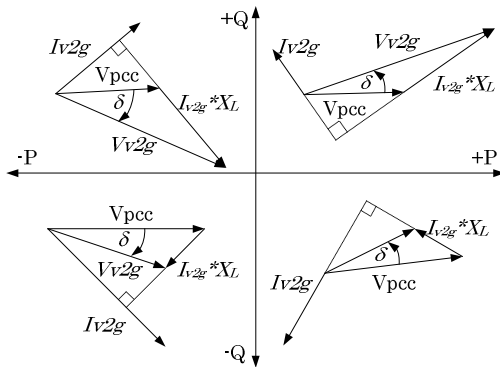

Figure 2 Operating modes of the V2G system.

To independently control real and reactive power, the Park's transformation (Schauder and

Mehta, 1991) is applied to transform all elements in the 3-phase AC coordinate to dq0 coordinate. From (6), the transformation result is shown in (7), where, VDC is the DC-link voltage.

$$\frac{d}{dt}\begin{bmatrix} I_d \\ I_q \end{bmatrix} = \begin{bmatrix} 0 & \omega \\ -\omega & 0 \end{bmatrix}\begin{bmatrix} I_d \\ I_q \end{bmatrix} + \frac{1}{L}\begin{bmatrix} v_d V_{DC} - |V_{pcc}| \\ v_q V_{DC} \end{bmatrix} \quad (7)$$

As (7), I_{v2g} can be considered by I_d and I_q as the active and reactive power command, respectively. These current can be controlled by the V2G voltage in dq0 coordinate, $v_d V_{DC}$ and $v_q V_{DC}$. At this point, the control state space of the V2G modeling can be expressed by

$$v_d V_{DC} = \left(k_p + \frac{k_i}{s} \right)\left(i_d^* - i_d \right) - \omega L i_q + |V_{pcc}| \quad (8)$$

$$v_q V_{DC} = \left(k_p + \frac{k_i}{s} \right)\left(i_q^* - i_q \right) + \omega L i_d \quad (9)$$

where, k_p is the proportional gain,

k_i is the integral gain,

i_d^* is the command current of active power,

i_q^* is the command current of reactive power,

$|V_{pcc}|$ is amplitude of the PCC voltage,

L is inductance of the coupling inductor.

This control state space expressed by (8) and (9) also known as the DQ synchronous

reference frame control (Schauder and Mehta, 1991), and can be illustrated by the block diagram in (Figure 3).

The study power distribution network

　　　In this research, the study power distribution network is shown in (Figure 4). It is a simple 3-phase radial low-voltage feeder, where the V2G system has penetrated into the PCC1 through PCC6 locations. For the parameters are summarized in the (Table 3).
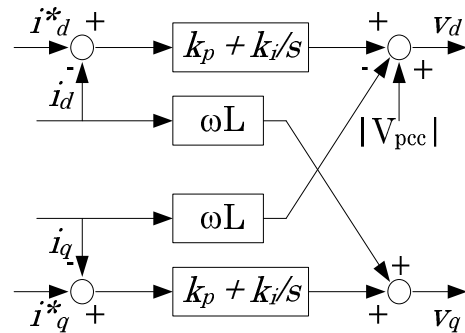

Figure 3 DQ synchronous reference frame control.
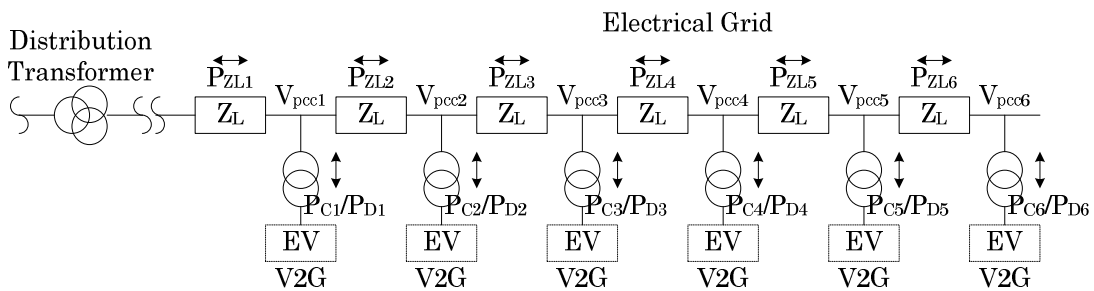
Figure 4 The study power distribution network.

Table 3 Parameters of the study power distribution network.

parameters	variable	unit
line impedance	Z_L	0.67%
nominal PCC voltage (peak)/phase	V_{Peak}	311 V (220 Vrms)
coupling inductor	L	5 mH
rated charging/discharging power	P_C, P_D	±10 kW

The case study of V2G penetration

　　　The case study of the V2G penetration can be considered by 3 cases: for Case 1, the amounts of active power are charging (P_C) and discharging (P_D) in a same rate. But for Case 2 and Case 3, an amount of active power is charging more and less than discharging, respectively. The purpose of Case1 and Case 3 is to describe the scenario that the amount of discharging power from the V2G system can

serve enough the load demand in the power distribution network, and possibly reverse the amount of discharge power back to the main power network. These scenarios is similar to the virtual power plant (VPP) in which the V2G system is operated as the distributed generator (DG) continues to power a location even though electrical grid power from the electric utility is no longer present, and also can possibly reverse the amount of discharge power back to the grid utility. For the Case 2, the purpose is to describe a normal demand in the system.

For the following, the power losses, voltage variation, and the probability of the V2G location in the study network are analyzed in order to investigate the relationship among the power losses, voltage variation, and the V2G location. In this research, the studied cases are modeled and simulated by the MATLAB Simulink software. The details of an analysis are provided in the simulation results section.

Results and discussion

Before the V2G penetration, the initial PCC voltages of VPCC1 through VPCC6 are equal to the nominal PCC voltage as summarized in (Table 3). After the V2G penetration, these voltages will be varied, and the line power losses due to the power flow will be occurred corresponding to the probability

charging or discharging location of the V2G system. Simulation results of the Case 1, Case 2, and Case 3 have shown in (Table 4-6), respectively. For the Case 1, it can be found that the maximum power losses by the line impedance (0.67% of the minimum load impedance), P_{ZL1} through P_{ZL6}, are occurred when the congestion of discharging power by the V2G is located close to the distribution transformer or the end of feeder. This is due to the large amount of discharging current have injected into- or drawn from the end of feeder to serve for the P_D. These current have also made the voltage drastically dropped and raised following the behavior above.

For the Case 2, the drastically raised of the voltage at the end of feeder (V_{PCC6}) is not occurred due to the congestion of discharging power at the end of feeder. This is because both active power from the power distribution network and the V2G system have served for the P_D at the end of feeder. However, the maximum power losses are occurred when the congestion of discharging power by the V2G is located close to the distribution transformer. For the Case 3, on the contrary, the maximum power losses have been found when the congestion of discharging power by the V2G is located close to the end of feeder, but the drastically dropped of the voltage at the end of feeder is not found when the congestion of discharging power is located close to the

distribution transformer. This is due to the V2G can both serve for the P_D and inject active power reverse to the distribution transformer.

For another location, the line power losses can be analyzed with the proposed variation index. The variation index is obtained by the mean (*M.*) multiplied with standard deviation (*S.D.*) and divided by range (*R.*). For the variation index calculation, the variation value of location from the distribution transformer to the end of feeder can be set as the number, for example by PCC1 is "1", PCC6 is "6". The relationships between the line power losses and the variation index can be illustrated in (Figure 5). For Case 1, the trend of power losses is similar to the U-curve. It can be found large amount of power losses when the variation index is minimum or maximum value. For Case 2 the trend of power losses is similar to the x^2-curve, where the amount of power losses is high when the variation index is increased. For the case 3, on the contrary, the trend of power losses is similar to the $1/x^2$-curve, where the amount of power losses is low when the variation index is decreased.

(a)

(b)

(c)
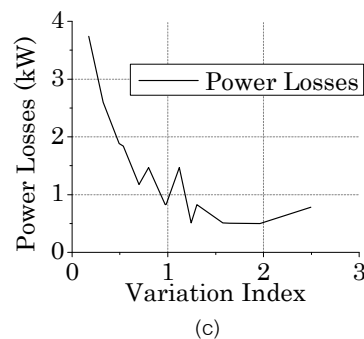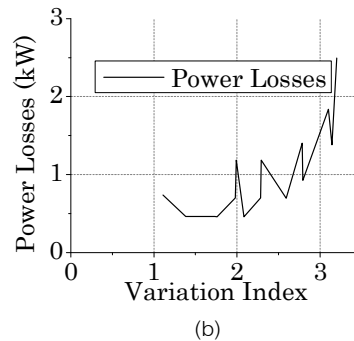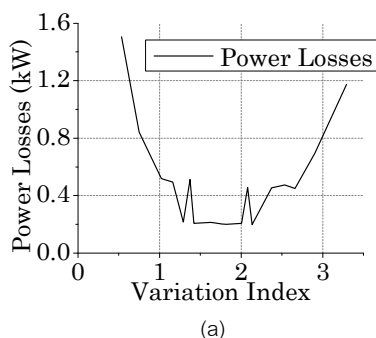
Figure 5 Power losses and the variation index by (a) Case 1, (b) Case 2, and (c) Case 3.

Conclusion

This research analyzes the line power losses and voltage variation that are caused by the V2G system penetration in the study power network. Overview of the electric vehicles type, standards, and the V2G concept are provided. The V2G system is demonstrated as mathematical model, and simulated by the computer program for investigating the relationship among the line power losses, voltage variation, and probability of the V2G location. The 3 cases study of the V2G penetrations are present and assign to describe the behavior of

charging and discharging the amount of active power by the V2G system. The simulation results show large amount of line power losses and voltage variation issues can be found in case of the congestion of discharging an amount of active power is closely occurred to the distribution transformer and the end of power distribution network. However, these issues can be overcome by distributing the charging or discharging location of the V2G system. The relationship earlier mentioned can clearly depict by the proposed variation index. The variation index can be useful for location optimization research. For the further work, the complicated power distribution network will be studied.

Table 4 The PCC voltage and line power losses by charging and discharging of V2G system for Case 1.

P_{ZL1}(W)	Vpcc1	P_{ZL2}(W)	Vpcc2	P_{ZL3}(W)	Vpcc3	P_{ZL4}(W)	Vpcc4	P_{ZL5}(W)	Vpcc5	P_{ZL6}(W)	Vpcc6	P_{ZT}(W)
1	311	91	308	321	304	698	297	314	292	79	290	1,505
0	311	81	309	301	304	79	302	304	297	76	295	841
0	311	76	309	292	304	74	302	0	302	74	300	516
0	311	76	309	292	304	74	302	0	302	72	304	513
0	311	76	309	0	309	76	306	294	302	74	300	521
0	311	72	309	0	309	72	307	0	307	72	305	215
0	311	71	309	0	309	72	307	0	307	70	309	213
0	311	71	309	0	309	68	311	0	311	70	309	210
0	311	75	309	0	309	65	311	267	315	66	317	474
0	311	71	309	0	309	68	311	0	311	68	313	208
1	311	54	313	244	317	565	323	248	327	62	329	1,173
0	311	60	313	256	317	62	319	254	323	63	325	695
0	311	63	313	262	317	65	319	0	319	65	321	455
0	311	63	313	262	317	65	319	0	319	66	317	456
0	311	63	313	0	313	63	315	260	319	63	321	450
0	311	67	313	0	313	66	315	0	315	66	317	199
0	311	67	313	0	313	66	315	0	315	68	313	201
0	311	67	313	0	313	70	311	0	311	68	313	204
0	311	63	313	0	313	74	311	286	306	72	304	495
0	311	66	313	0	313	70	311	0	311	70	309	206

Table 5 The PCC voltage and line power losses by charging and discharging of V2G system for Case 2.

P$_{ZL1}$(W)	Vpcc1	P$_{ZL2}$(W)	Vpcc2	P$_{ZL3}$(W)	Vpcc3	P$_{ZL4}$(W)	Vpcc4	P$_{ZL5}$(W)	Vpcc5	P$_{ZL6}$(W)	Vpcc6	P$_{ZT}$(W)
387	306	791	299	1,352	289	775	282	350	277	88	275	3,743
351	306	738	299	344	295	746	288	336	283	85	280	2,599
328	307	704	300	321	295	84	293	324	288	82	286	1,842
317	307	688	300	310	295	79	293	0	293	79	291	1,472
317	307	688	300	310	295	79	293	0	293	77	295	1,469
329	306	94	304	332	299	721	292	325	288	82	285	1,882
308	307	83	304	311	300	81	297	313	293	79	291	1,175
298	307	78	304	300	300	76	298	0	298	76	295	829
298	307	78	304	300	300	76	298	0	298	74	300	827
298	307	78	304	0	304	79	302	303	298	76	295	835
289	307	74	305	0	305	74	302	0	302	74	300	510
289	307	74	305	0	305	74	302	0	302	72	304	508
289	307	74	305	0	305	70	307	0	307	72	304	504
289	307	74	305	0	305	70	307	0	307	70	309	502
297	307	78	304	0	304	66	306	275	311	68	313	784

Table 6 The PCC voltage and line power losses by charging and discharging of V2G system for Case 3.

P$_{ZL1}$(W)	Vpcc1	P$_{ZL2}$(W)	Vpcc2	P$_{ZL3}$(W)	Vpcc3	P$_{ZL4}$(W)	Vpcc4	P$_{ZL5}$(W)	Vpcc5	P$_{ZL6}$(W)	Vpcc6	P$_{ZT}$(W)
212	315	518	321	949	329	527	335	232	339	58	340	2,495
228	315	543	321	233	325	538	331	237	335	59	337	1,838
239	315	560	321	244	325	59	327	242	331	60	333	1,404
245	315	568	321	250	325	62	327	0	327	62	329	1,186
245	315	568	321	250	325	62	327	0	327	63	325	1,187
240	315	53	317	238	321	551	327	242	331	60	333	1,384
252	315	59	317	250	321	60	323	248	327	62	329	929
258	315	62	317	256	321	63	323	0	323	63	326	701
258	315	62	317	256	321	63	323	0	323	65	321	703
258	315	62	317	0	317	62	319	254	323	63	325	698
264	315	65	317	0	317	65	319	0	319	65	322	458
264	315	65	317	0	317	65	319	0	319	66	317	460
264	315	65	317	0	317	68	315	0	315	66	317	463
264	315	65	317	0	317	68	315	0	315	68	313	464
257	315	61	317	0	317	72	315	278	311	70	309	738

▨ is discharging mode.   ☐ is charging mode.

References

Dehaghani, E.S. and S.S. Williamson. 2012. On the Inefficiency of vehicle-to-grid (V2G) power flow: Potential barriers and possible research directions. *IEEE Transportation Electrification Conference and Expo (ITEC), 2012 IEEE:* 1-5.

IEA (International Energy Agency). 2013. Global EV outlook 2013-understanding the electric vehicle landscape to 2020, Clean Energy Ministerial, and Electric Vehicles Initiative, International Energy Agency, April.

Kong, P.Y. and G.K. Karagiannidis. 2016. Charging schemes for plug-in hybrid electric vehicles in smart grid: A survey. *IEEE Access. 4:* 6846-6875.

Liu, C., K.T. Chau, D. Wu and S. Gao. 2013. Opportunities and challenges of vehicle-to-home, vehicle-to-vehicle, and vehicle-to-grid technologies. *Proceedings of the IEEE. 101(11):* 2409-2427.

Cleveland, C.J. and C. Morris. 2006. Dictionary of energy. Elsevier, Amsterdam.

Schauder, C. and H. Mehta. 1991. Vector analysis and control of advanced static VAR compensators. pp. 266-272. *In:* Conference Publication no. 345 of the IEE Fifth International Conference on AC and DC Power Transmission, September 1991. London, UK.

Sortomme, E. and M.A. El-Sharkawi. 2012. Optimal scheduling of vehicle-to-grid energy and ancillary services. *IEEE Transactions on Smart Grid. 3(1):* 351-359.

Zhu, J. 2015. Operation of smart grid, Optimization of power system operation, ch. 14, Wiley-IEEE Press.